Supporting Information

Achieving a high open-circuit voltage of 1.339 V in 1.77-eV wide-bandgap perovskite solar cells via self-assembled monolayers

Zongjin Yi[1,†], Wanhai Wang[2,3,†], Rui He[1], Jingwei Zhu[1], Wenbo Jiao[1], Yi Luo[1], Yuliang Xu[1], Yunfan Wang[4], Zixin Zeng[4], Kun Wei[5], Jinbao Zhang[5], Sai-Wing Tsang[4], Cong Chen[1], Weihua Tang[2,3,*], Dewei Zhao[1,*]

[1]College of Materials Science and Engineering & Engineering Research Center of Alternative Energy Materials & Devices, Ministry of Education, Sichuan University, Chengdu 610065, China

[2]Institute of Flexible Electronics (IFE, Future Technologies), College of Materials, Innovation Laboratory for Sciences and Technologies of Energy Materials of Fujian Province (IKKEM), Xiamen University, Xiamen 361005, China

[3]School of Chemistry and Chemical Engineering, Nanjing University of Science and Technology, Nanjing 210094, China

[4]Department of Materials Science and Engineering, City University of Hong Kong, 83 Tat Chee Ave, Kowloon Tong, Hong Kong SAR, China

[5]College of Materials, Fujian Key Laboratory of Advanced Materials, Xiamen Key Laboratory of Electronic Ceramic Materials and Devices, Xiamen University, Xiamen, China

*Correspondence to: dewei_zhao@hotmail.com and whtang@xmu.edu.cn
†These authors contributed equally.

Experimental Part

Materials

N, N-dimethylformamide (DMF), dimethyl sulfoxide (DMSO), toluene (TL), and $Pb(SCN)_2$ were purchased from Sigma-Aldrich. Diethyl ether (DE), anhydrous ethanol, and isopropanol (IPA) were purchased from Chengdu Chron Chemical Co., Ltd. Lead iodide (PbI_2) and lead bromide ($PbBr_2$) was purchased from TCI. Formamidinium iodide (FAI) was purchased from Greatcell Solar Company. Cesium iodide (CsI) was purchased from Alfa Aesar. Ploy(bias(4-phenyl)(2,4,6-trimethylphenyl)amine) (PTAA) was purchased from Xi'an Polymer Light Technology Corporation. C_{60} was purchased from Nano-C. BCP was purchased from Jilin OLED. Copper (Cu) was purchased from Zhongnuoxincai Co., Ltd. DCB-BPA is synthesized according to our previous work.[1]

Device preparation

Patterned indium tin oxide (ITO) glass substrates (25×25 mm, 10 Ω sq^{-1}) were sequentially cleaned with detergent, deionized water, and ethanol for 15 min at each procedure in an ultrasonic bath. Before the spin-coating of HTLs, ITO glass substrates were dried by a nitrogen flow and then treated with ultraviolet ozone for 15 min. For PTAA-based devices, PTAA dissolved in toluene with a concentration of 2 mg/mL was spin-coated at 4000 rpm for 30 s and then heated on a hot plate at 100 ℃ for 10 min. For SAM-based devices, DCB-BPA was dissolved in anhydrous ethanol with a concentration of 0.1, 0.2, and 0.4 mg/mL, respectively. The DCB-BPA solution was spin-coated at 3000 rpm for 20 s and heated at 120 ℃ for 10 min. The $FA_{0.8}Cs_{0.2}PbI_{1.8}Br_{1.2}$ perovskite precursor was prepared by dissolving 3.876 mg $Pb(SCN)_2$, 62.4 mg CsI, 165.12 mg FAI, 264.24 mg $PbBr_2$, 221.28 mg PbI_2 in 1 ml mixed solvent of DMF and DMSO with a volume ratio of 3:1 and stirred at 60 ℃ for 3 h before use. For the preparation of complete devices, 80 μL of perovskite precursor was dropped on the substrate and spin-coated through a two-step process, i.e., 500 rpm for 2 s and then 4000 rpm for 60 s. At the second stage, 700 μL of diethyl ether was dropped after the spin-coating of 25 s. The as-prepared perovskite film was annealed at 60 ℃ for 3 min and 100 ℃ for 10 min. Then the perovskite films were treated by a TEACl solution dissolved in IPA with a concentration of 2 mg/mL at 3000 rpm for 30 s, and then followed by an additional annealing process at 100 ℃ for 5 min according to our previous work.[2] After a short cooling, all samples were transferred into a thermal evaporation chamber, and a 20 nm C_{60} layer was evaporated at 5×10^{-4} Pa. For the opaque device, 5nm BCP and 100 nm Cu was

thermally evaporated in an evaporation chamber with a vacuum degree of 5×10-4 Pa. For the semitransparent device, the deposition of ALD-SnO_2 was performed using tetrakis(dimethylamino) tin (IV) and deionized water as precursors. And, 180 nm IZO was sputtered at 70 W power at a pressure of 0.2 Pa. 1.25-eV narrow bandgap perovskite solar cells were fabricated according to our previous work.[3] The active area of the device is 0.0975 cm^2, defined by the overlapped region between the back electrode and the ITO substrate.

Analysis Methods

Film Characterization: XPS measurement was performed by a photoelectron spectrometer (ThermoFischer, ESCALAB Xi +) with Al-Kα radiation (hν = 1486.6 eV) at 12.5 kV and 16 mA. Contact angles of PTAA and DCB-BPA were measured by a contact angle analyzer (JY-82B Kruss DSA). Scanning electron microscope (SEM) images were taken by Hitachi S-5200 microscope with an acceleration voltage of 10 kV. Powder X-ray diffraction (XRD) data were obtained using a Shimazu XRD-6100 diffractometer with Cu-Kα radiation (λ = 1.5406 Å) at 40 kV and 30 mA. PL and TRPL measurements of perovskite films were performed by FLS980 (Edinburgh Inc) with a 532 nm wide spectrum light source as the excitation light source. Ultraviolet Photoelectron Spectroscopy (UPS) was performed by PHI 5000 VersaProbe III with He I source (21.22 eV) under an applied negative bias of 9.0 V.

Details of the PVSK exfoliation: Exfoliation of the perovskite films: PMMA (Sigma-Aldrich) precursor was prepared by dissolving 0.4g PMMA in 1mL CB. Epoxy precursor was prepared by mixing diglycidyl ether bisphenol A type (Sigma-Aldrich), n-octylamine (Sigma-Aldrich) and m-xylylenediamine (Sigma-Aldrich) with a molar ratio of 4:2:1. PMMA and epoxy layer were blade coated on the perpated perovskite film in a sequential order. In order to accelerate the cross-link process of epoxy, the coated substrate was annealed at 70 °C for 10 min. After 12 hours, the epoxy was completely solidified at room temperture. Finally, perovskite film was exfoliated from glass/ITO substrate by a glass nipping plier.The micro-morphology of perovskite films bottom surface was characterized by SEM (SU-70, Japan Hitachi Nake high-tech enterprise). PL intensity (680 nm) mapping were obtained by Vis-NIR-XU (Nanophoton Corporation) with an excitation at 532 nm.

Device Characterization: *J-V* curves were recorded by a Keysight Technologies B2901A source meter under simulated solar illumination (Enlitech, SS-F5-3A). The light intensity was calibrated by a silicon reference cell (SRC-00205, Enlitech). The scan rate for *J-V* measurement was 100 $mV \cdot s^{-1}$, with a delay time of 100 ms and a voltage step of 10 mV. All

devices were tested using a shadow mask with an active area of 0.0576 cm^2 for opaque devices and 0.0624 cm^2 for semitransparent devices. S-Q limit calculations were performed using a freely available Python code.[4] The light intensity dependence of V_{OC} was obtained by measuring *J-V* curves under different illumination intensities. The EQE spectra were measured under monochromatic light ranging from 300 nm to 800 nm with a 10 nm increment and a chopper frequency of 210 Hz via a QE system (QE-R, Enli Tech). The MPP of the encapsulated devices were tracked by an LED (Guangzhou Crysco Equipment Co., Ltd.) under the relative humidity of ~ 50%. The dark *J-V* and SCLC was measured with a Keysight Technologies B2901A source meter under dark conditions. EIS and *C-V* measurements were performed by an electrochemical workstation (IVIUMSTAT). For EIS measurement, the frequency was changed from 10^8 Hz to 1000 Hz at the bias of 1.1 V with an amplitude of 20 mV. For C-V measurement, the frequency was fixed at 1000 Hz with the voltage range of 0 V to 1.2 V. The highly-sensitive external quantum efficiency (s-EQE) spectra of wide-bandgap perovskite solar cells were obtained by using a home-built setup. During the measurements, light from a 1000 W xenon arc lamp (Newport) passes through a monochromator (Zolix) and optical chopper (ThorLabs) before being focused on the device active area. The generated photocurrent was amplified by a current amplifier (Standard Research SR570) and then collected by a lock-in amplifier (Standard Research SR830). The intensity of the light source was measured by calibrated silicon and germanium detectors (ThorLabs). EL was measured by Enlitech REPS with a bias from 0.5 V to 2.5 V.

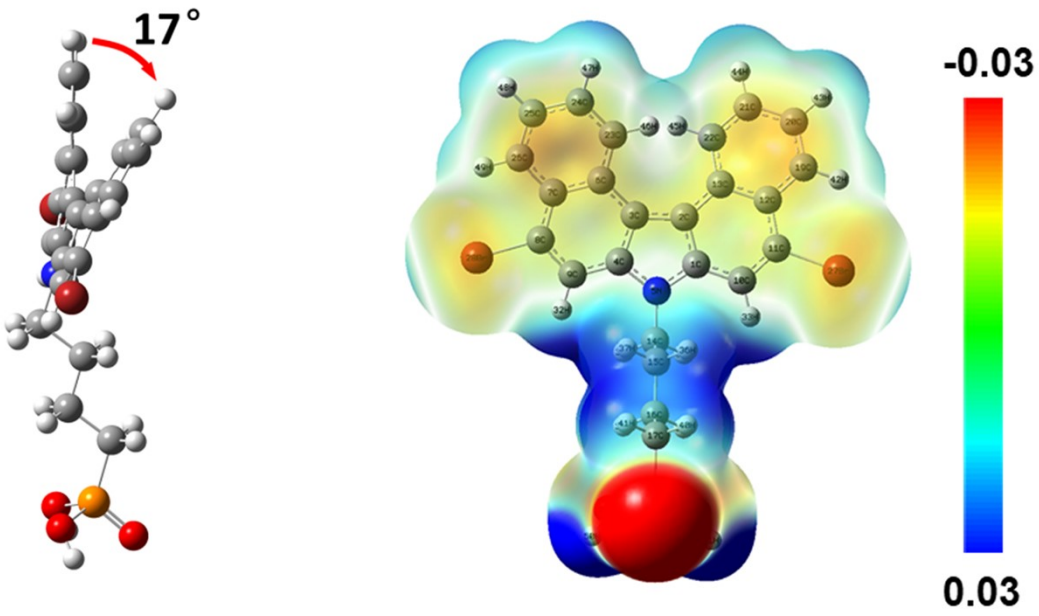

Figure S1. Side view and electrostatic surface potential of DCB-BPA.

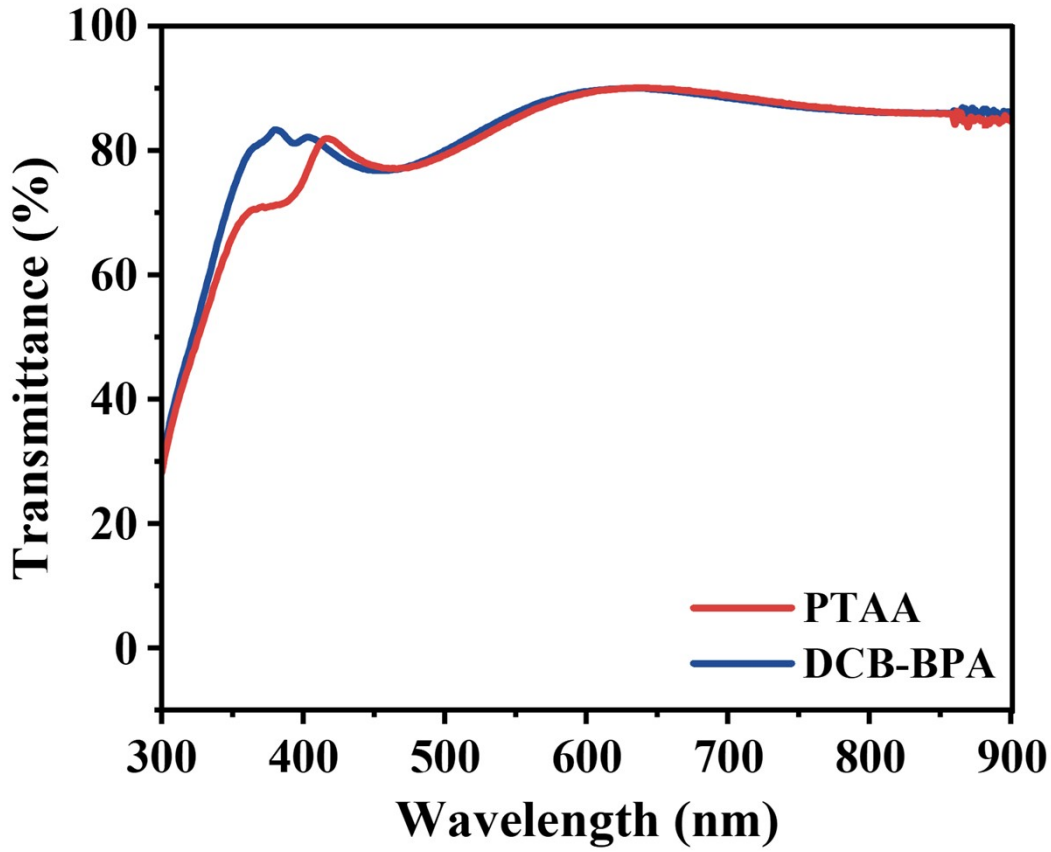

Figure S2. Transmittance spectra of PTAA/ITO and DCB-BPA/ITO.

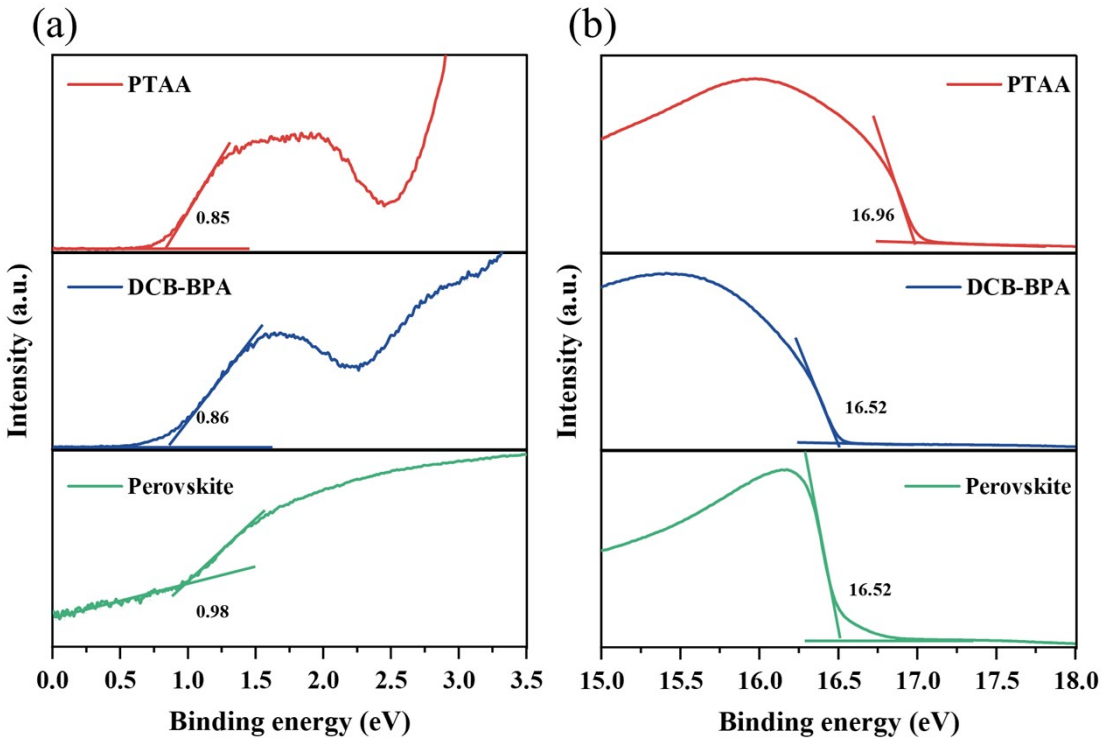

Figure S3. Valence band edge (a) and secondary electron cut-off edge (b) from UPS measurements of different HTLs and the 1.77-eV WBG perovskite.

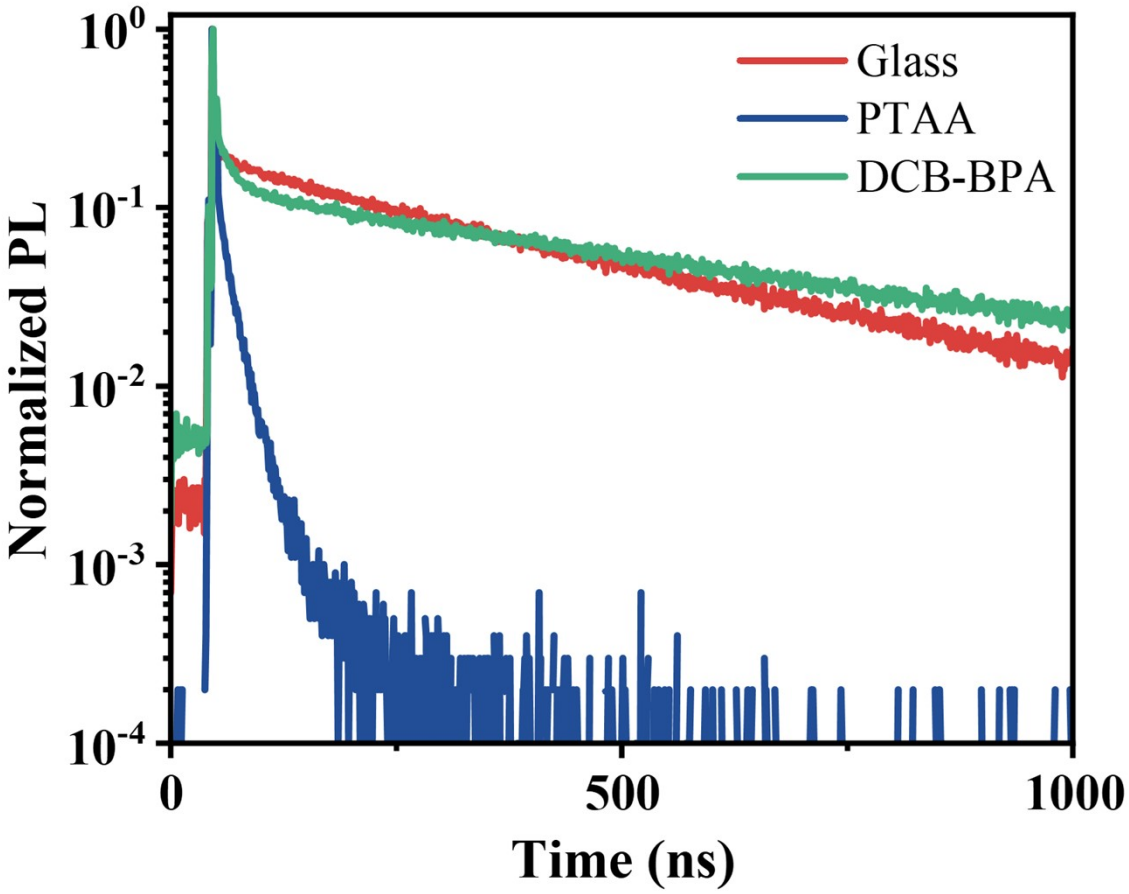

Figure S4. TRPL decays of perovskite films deposited on glass, PTAA, and DCB-BPA.

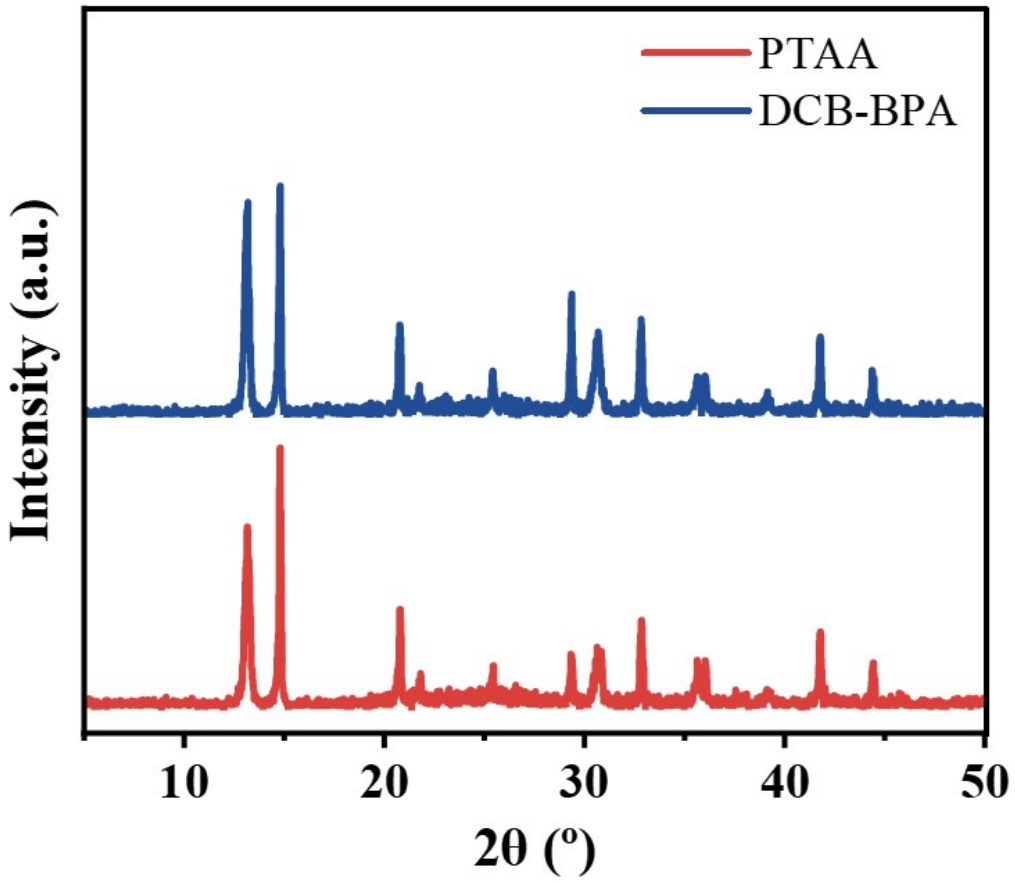

Figure S5. XRD patterns of WBG perovskite films deposited on PTAA and DCB-BPA.

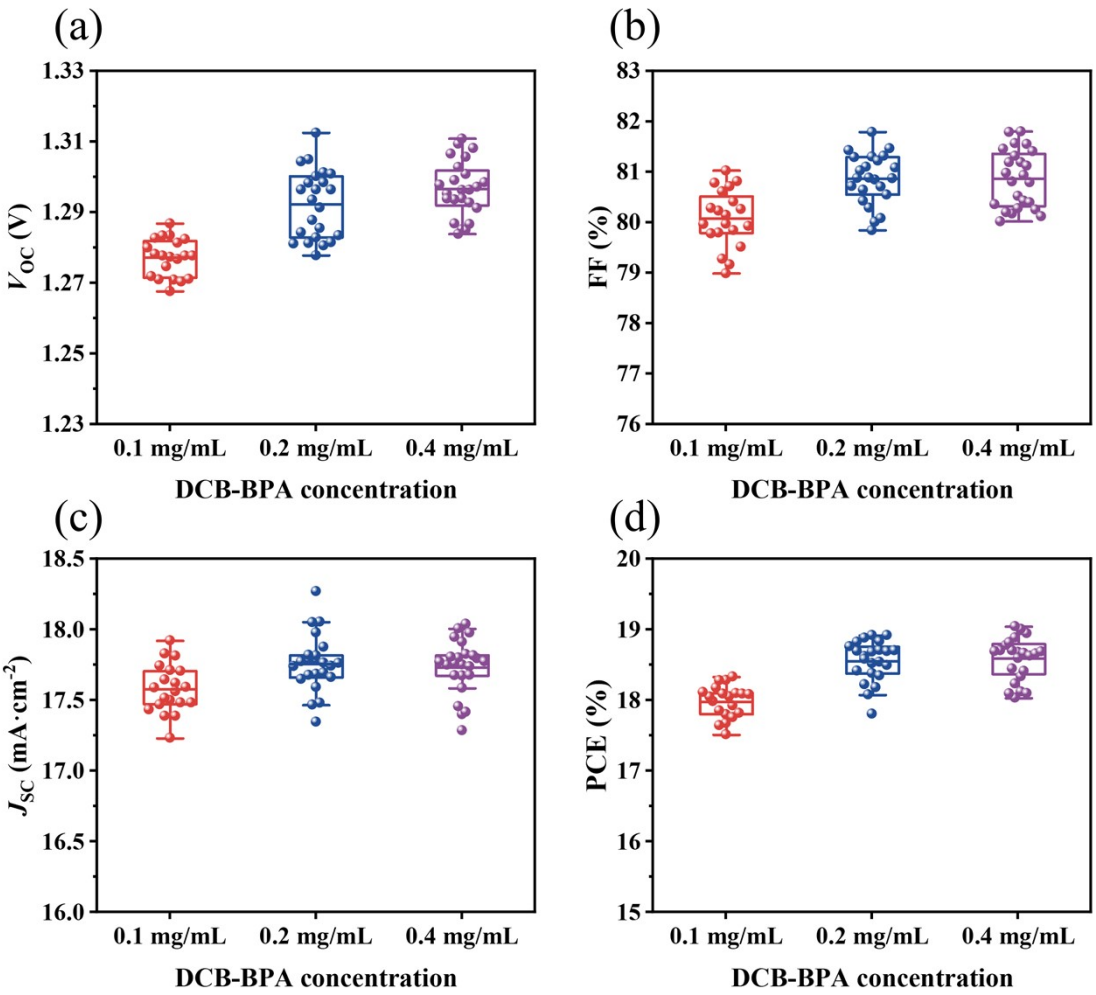

Figure S6. Statistics of photovoltaic parameters of devices with different concentrations of DCB-BPA. (a) V_{OC}, (b) FF, (c) J_{SC}, and (d) PCE.

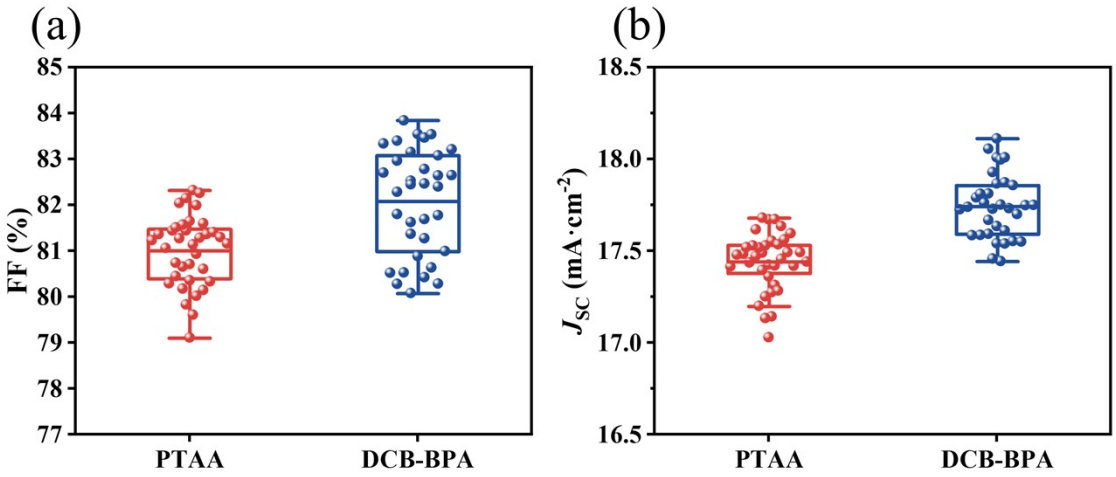

Figure S7. Statistics of photovoltaic parameters of devices with PTAA and DCB-BPA as HTLs. (a) FF and (b) J_{SC}.

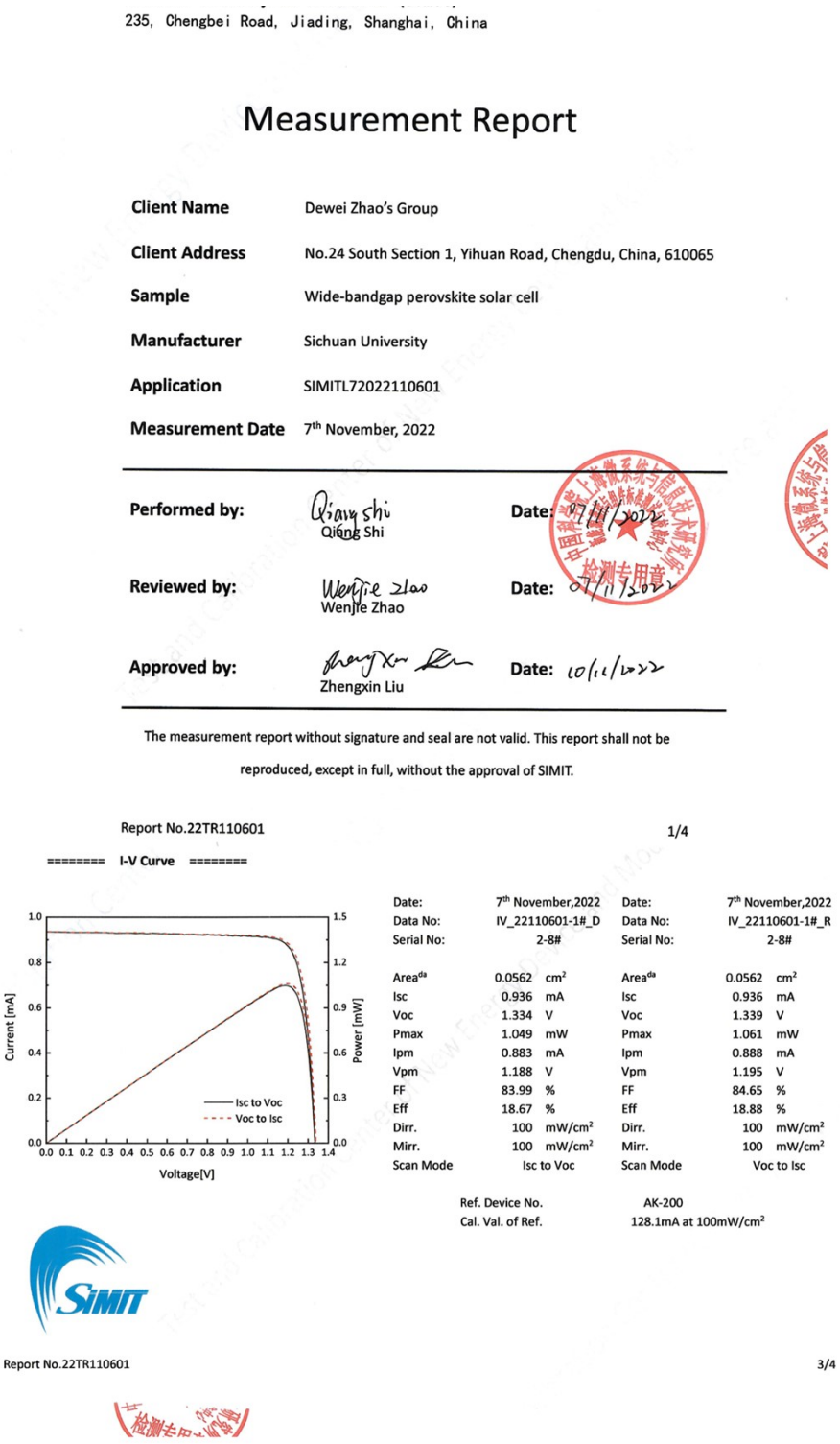

235, Chengbei Road, Jiading, Shanghai, China

Measurement Report

Client Name	Dewei Zhao's Group
Client Address	No.24 South Section 1, Yihuan Road, Chengdu, China, 610065
Sample	Wide-bandgap perovskite solar cell
Manufacturer	Sichuan University
Application	SIMITL72022110601
Measurement Date	7th November, 2022

Performed by: Qiang Shi **Date:** 7/11/2022

Reviewed by: Wenjie Zhao **Date:** 8/11/2022

Approved by: Zhengxin Liu **Date:** 10/11/2022

The measurement report without signature and seal are not valid. This report shall not be reproduced, except in full, without the approval of SIMIT.

Report No.22TR110601 1/4

======== I-V Curve ========

Date:	7th November,2022		Date:	7th November,2022	
Data No:	IV_22110601-1#_D		Data No:	IV_22110601-1#_R	
Serial No:	2-8#		Serial No:	2-8#	
Area^{da}	0.0562	cm^2	Area^{da}	0.0562	cm^2
Isc	0.936	mA	Isc	0.936	mA
Voc	1.334	V	Voc	1.339	V
Pmax	1.049	mW	Pmax	1.061	mW
Ipm	0.883	mA	Ipm	0.888	mA
Vpm	1.188	V	Vpm	1.195	V
FF	83.99	%	FF	84.65	%
Eff	18.67	%	Eff	18.88	%
Dirr.	100	mW/cm^2	Dirr.	100	mW/cm^2
Mirr.	100	mW/cm^2	Mirr.	100	mW/cm^2
Scan Mode	Isc to Voc		Scan Mode	Voc to Isc	

Ref. Device No. AK-200

Cal. Val. of Ref. 128.1mA at 100mW/cm^2

Report No.22TR110601 3/4

Figure S8. Measurement report of a WBG PSC certified by Shanghai Institute of Microsystem and Information Technology. The device has an independently certified PCE of 18.88% (18.67%) under reverse (forward) voltage scan.

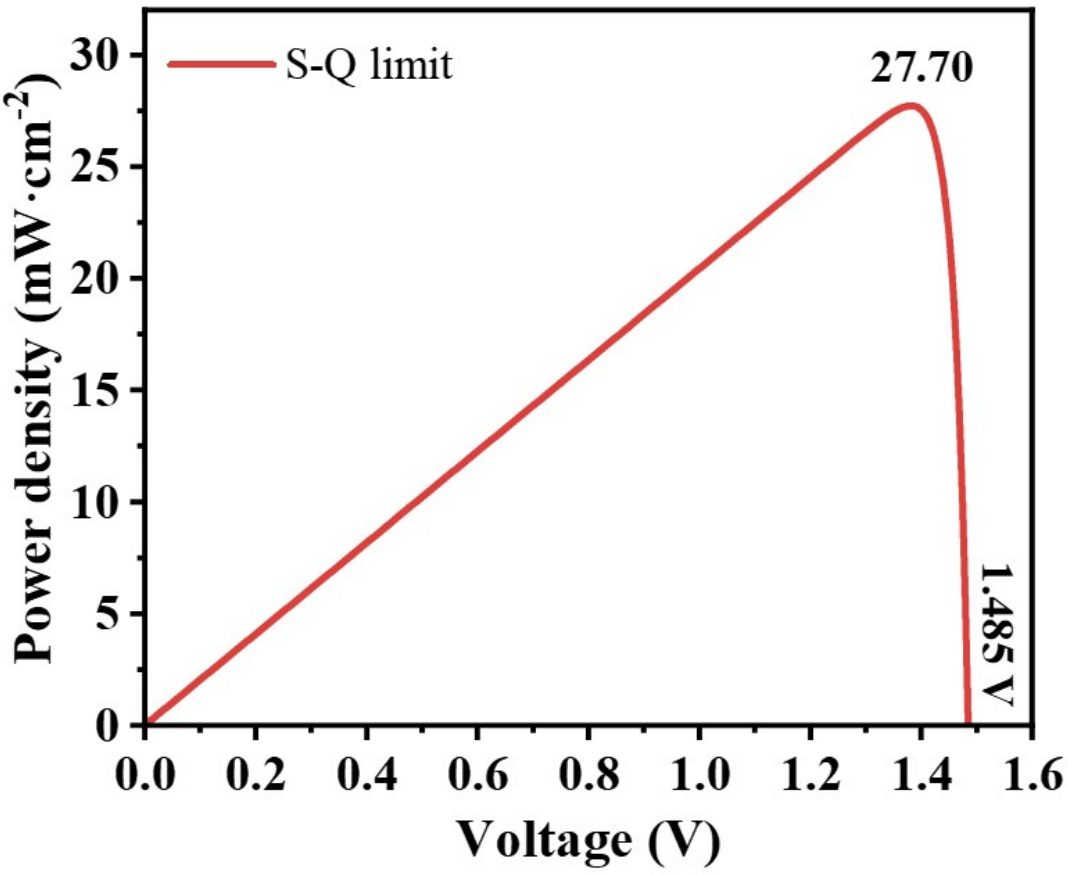

Figure S9. *P-V* curves of S-Q limit of 1.77-eV PSCs.[4]

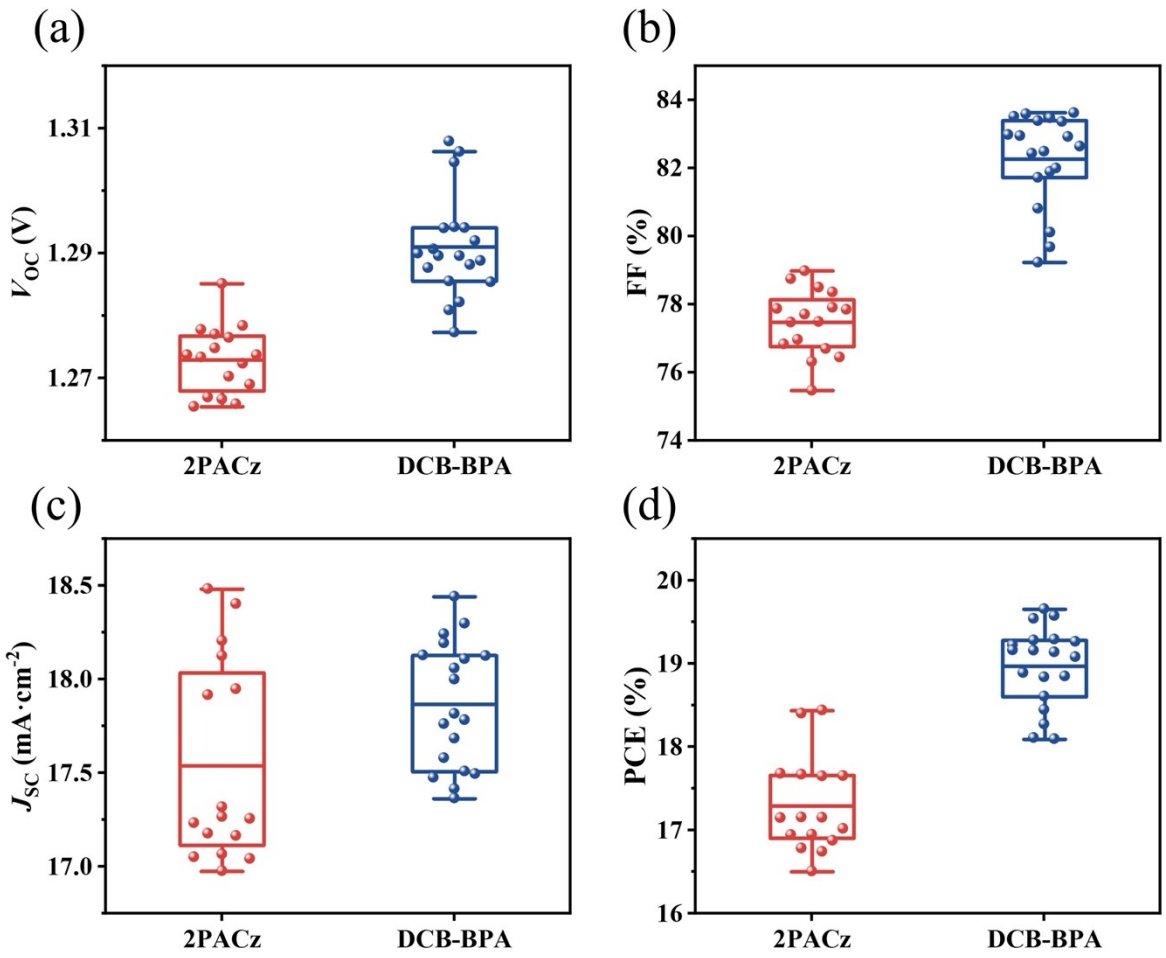

Figure S10. Statistics of photovoltaic parameters of devices with 2PACz and DCB-BPA as HTLs. (a) V_{OC}, (b) FF, (c) J_{SC} and (d) PCE

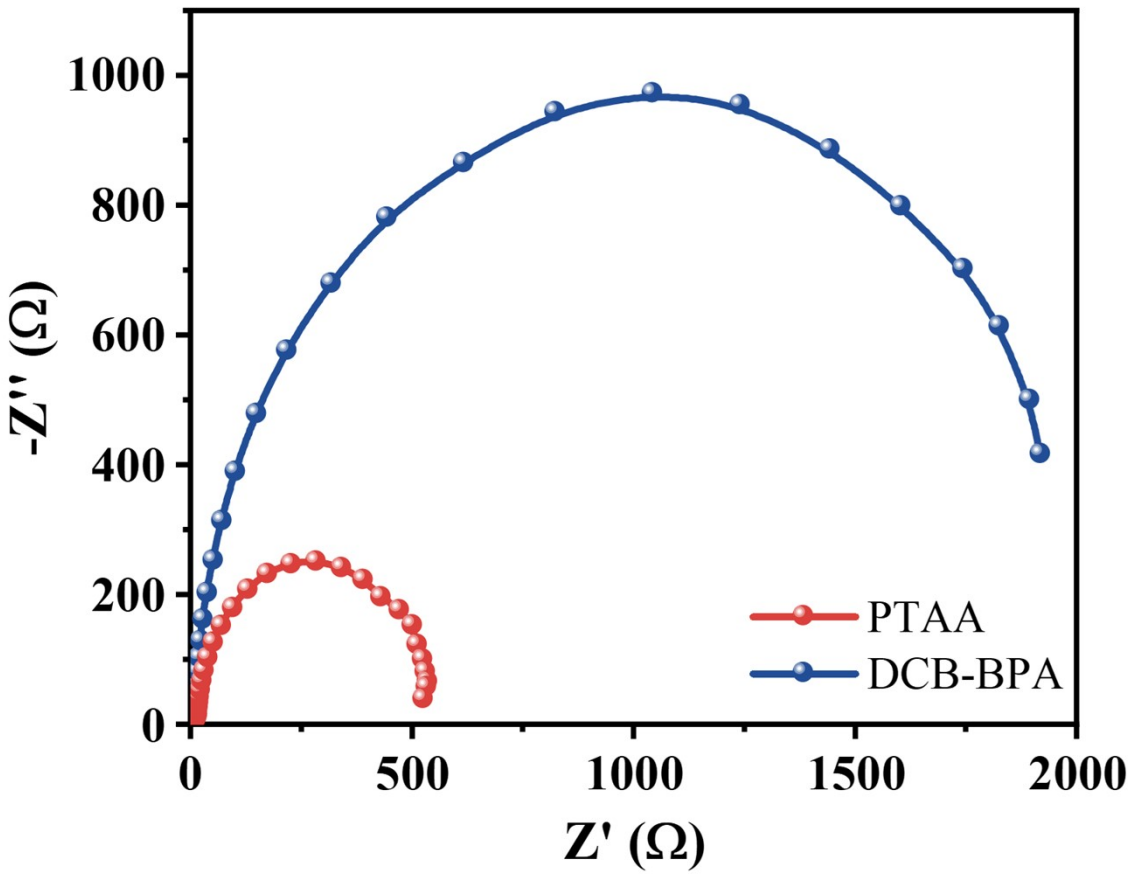

Figure S11. EIS of PTAA and DCB-BPA devices.

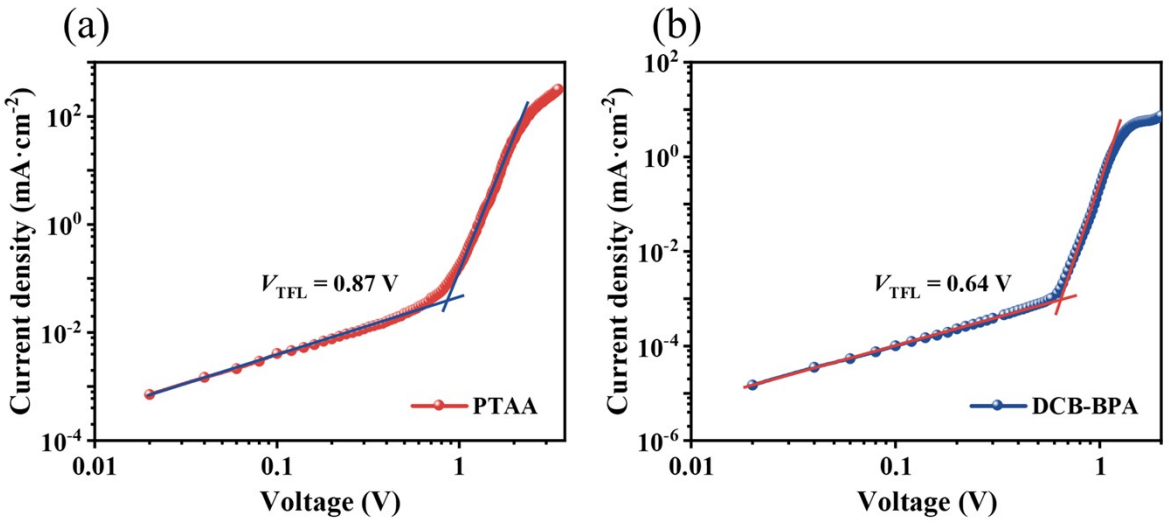

Figure S12. SCLC measurements of hole-only devices tailored by (a) PTAA and (b) DCB-BPA.

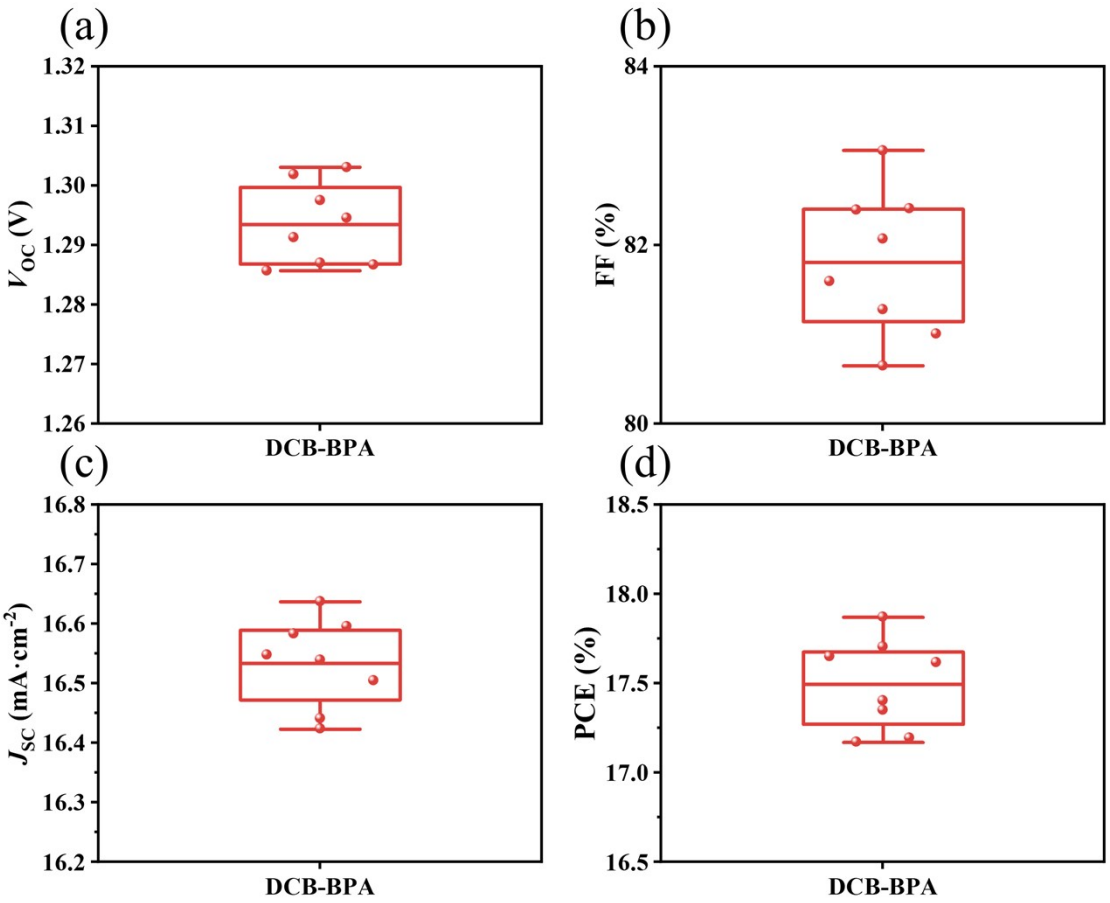

Figure S13. Statistics of photovoltaic parameters of semitransparent devices using DCB-BPA as HTL. (a) V_{OC}, (b) FF, (c) J_{SC}, and (d) PCE.

Table S1. Fitted data for TRPL decays of perovskite films on different HTLs.

	τ_1 (ns)	A_1	τ_2 (ns)	A_2	τ_{ave} (ns)
Glass	111	0.087	401	0.913	375
PTAA	11	0.606	28	0.394	18
DCB-BPA	19	0.034	584	0.966	564

Table S2. Photovoltaic parameters of champion devices using different HTLs under forward and reverse voltage scans.

HTL	V_{OC} (V)	FF (%)	J_{SC} (mA·cm^{-2})	PCE (%)
PTAA (forward)	1.20	80.69	17.67	17.08
PTAA (reverse)	1.20	81.28	17.67	17.22
DCB-BPA (forward)	1.33	82.42	17.80	19.52
DCB-BPA (reverse)	1.33	82.70	17.75	19.53

Table S3. Photovoltaic performance metrics of state-of-the-art p-i-n WBG (> 1.75 eV) PSCs.

Year	Device structure	E_g (eV)	V_{OC} (V)	V_{OC} loss (mV)	PCE (%)	Ref.
2019	p-i-n	1.75	1.24	510	18.19	[5]
2019	p-i-n	1.81	1.21	600	17.1	[6]
2020	p-i-n	1.75	1.26	490	18.3	[7]
2022	p-i-n	1.79	1.25	540	17.6	[8]
2022	p-i-n	1.79	1.26	530	17.8	[9]
2022	p-i-n	1.8	1.26	540	17.7	[10]
2022	p-i-n	1.77	1.284	486	17.72	[11]
2022	p-i-n	1.75	1.33	420	20.3	[12]
2023	p-i-n	1.79	1.33 (Certified)	460	19.3 (Certified)	[13]
2023	p-i-n	1.77	1.31 V (1 cm^2)	460	18.46 (1 cm^2)	[14]
2023	p-i-n	1.77	1.31	460	19.33	[15]
2023	p-i-n	1.77	1.32	450	19.85	[16]
This work	p-i-n	1.77	1.339 (Certified)	431	18.88 (Certified)	

Table S4. Photovoltaic parameters of devices used for the 4-T all-perovskite tandem cell.

	V_{OC} (V)	FF (%)	J_{SC} (mA·cm^{-2})	PCE (%)
Top cell	1.3	83.06	16.58	17.87
Bottom cell	0.86	77.04	31.00	20.53
Bottom cell (filtered)	0.82	79.76	13.85	9.03
4-T tandem cell	/	/	/	26.90

References

1. W. Wang, Z. Lin, S. Gao, W. Zhu, X. Song and W. Tang, *Adv. Funct. Mater.*, 2023, DOI: 10.1002/adfm.202303653.
2. C. Chen, J. Liang, J. Zhang, X. Liu, X. Yin, H. Cui, H. Wang, C. Wang, Z. Li, J. Gong, Q. Lin, W. Ke, C. Tao, B. Da, Z. Ding, X. Xiao and G. Fang, *Nano Energy*, 2021, **90**, 106608.
3. Q. Y. Chen, J. C. Luo, R. He, H. G. Lai, S. Q. Ren, Y. T. Jiang, Z. X. Wan, W. W. Wang, X. Hao, Y. Wang, J. Q. Zhang, I. Constantinou, C. L. Wang, L. L. Wu, F. Fu and D. W. Zhao, *Adv. Energy Mater.*, 2021, **11**, 2101045.
4. S. HAMADY, Python solar cell shockley-queisser limit calculator, https://github.com/sidihamady/Shockley-Queisser.
5. C. Chen, Z. Song, C. Xiao, D. Zhao, N. Shrestha, C. Li, G. Yang, F. Yao, X. Zheng, R. J. Ellingson, C.-S. Jiang, M. Al-Jassim, K. Zhu, G. Fang and Y. Yan, *Nano Energy*, 2019, **61**, 141-147.
6. Y. M. Xie, Z. Zeng, X. Xu, C. Ma, Y. Ma, M. Li, C. S. Lee and S. W. Tsang, *Small*, 2020, **16**, 1907226.
7. Z. Li, J. Zhang, S. F. Wu, X. Deng, F. Z. Li, D. J. Liu, C. C. Lee, F. Lin, D. Y. Lei, C. C. Chueh, Z. L. Zhu and A. K. Y. Jen, *Nano Energy*, 2020, **78**, 105377.
8. S. Qin, C. Lu, Z. Jia, Y. Wang, S. Li, W. Lai, P. Shi, R. Wang, C. Zhu, J. Du, J. Zhang, L. Meng and Y. Li, *Adv. Mater.*, 2022, **34**, 2108829.
9. W. Chen, Y. Zhu, J. Xiu, G. Chen, H. Liang, S. Liu, H. Xue, E. Birgersson, J. W. Ho, X. Qin, J. Lin, R. Ma, T. Liu, Y. He, A. M.-C. Ng, X. Guo, Z. He, H. Yan, A. B. Djurišić and Y. Hou, *Nat. Energy*, 2022, **7**, 229-237.
10. J. Wen, Y. Zhao, Z. Liu, H. Gao, R. Lin, S. Wan, C. Ji, K. Xiao, Y. Gao, Y. Tian, J. Xie, C. J. Brabec and H. Tan, *Adv. Mater.*, 2022, **34**, 2110356.
11. R. He, Z. Yi, Y. Luo, J. Luo, Q. Wei, H. Lai, H. Huang, B. Zou, G. Cui, W. Wang, C. Xiao, S. Ren, C. Chen, C. Wang, G. Xing, F. Fu and D. Zhao, *Adv. Sci.*, 2022, **9**, 2203210.
12. Q. Jiang, J. Tong, R. A. Scheidt, X. Wang, A. E. Louks, Y. Xian, R. Tirawat, A. F. Palmstrom, M. P. Hautzinger, S. P. Harvey, S. Johnston, L. T. Schelhas, B. W. Larson, E. L. Warren, M. C. Beard, J. J. Berry, Y. Yan and K. Zhu, *Science*, 2022, **378**, 1295-1300.
13. H. Chen, A. Maxwell, C. Li, S. Teale, B. Chen, T. Zhu, E. Ugur, G. Harrison, L. Grater, J. Wang, Z. Wang, L. Zeng, S. M. Park, L. Chen, P. Serles, R. A. Awni, B. Subedi, X. Zheng, C. Xiao, N. J. Podraza, T. Filleter, C. Liu, Y. Yang, J. M. Luther, S. De Wolf, M. G. Kanatzidis, Y. Yan and E. H. Sargent, *Nature*, 2023, **613**, 676-681.
14. R. He, W. Wang, Z. Yi, F. Lang, C. Chen, J. Luo, J. Zhu, J. Thiesbrummel, S. Shah, K. Wei, Y. Luo, C. Wang, H. Lai, H. Huang, J. Zhou, B. Zou, X. Yin, S. Ren, X. Hao, L. Wu, J. Zhang, J. Zhang, M. Stolterfoht, F. Fu, W. Tang and D. Zhao, *Nature*, 2023, **618**, 80-86.
15. J. Zhu, Y. Luo, R. He, C. Chen, Y. Wang, J. Luo, Z. Yi, J. Thiesbrummel, C. Wang, F. Lang, H. Lai, Y. Xu, J. Wang, Z. Zhang, W. Liang, G. Cui, S. Ren, X. Hao, H. Huang, Y.

Wang, F. Yao, Q. Lin, L. Wu, J. Zhang, M. Stolterfoht, F. Fu and D. Zhao, *Nat. Energy*, 2023, **8**, 714-724.

16. H. Liu, J. Dong, P. Wang, B. Shi, Y. Zhao and X. Zhang, *Adv. Funct. Mater.*, 2023, DOI: 10.1002/adfm.202303673.